Progress In Electromagnetics Research, PIER 59, 231–249, 2006

CONDUCTING SHEATH HELICAL WINDING ON THE CORE-CLADDING INTERFACE OF A LIGHTGUIDE HAVING A PIET HEIN SUPER ELLIPTICAL CORE CROSS-SECTION AND A STANDARD OPTICAL FIBER OF CIRCULAR CROSS-SECTION — A COMPARATIVE MODAL ANALYSIS

V. Singh

Department of Physics
University Institute of Engineering and Technology
C.S.J.M. University
Kanpur-208 024, [U.P.] India

S. N. Maurya

Department of Applied Physics
Institute of Engineering and Rural Technology
Allahabad, [U.P.] India

B. Prasad and S. P. Ojha

Department of Applied Physics
Institute of Technology
Banaras Hindu University
Varanasi-221005, [U.P.] India

Abstract—In this article, a theoretical and computational analysis has been made to obtain the modal dispersion characteristics of an unconventional optical waveguide with a Piet Hein core cross section having a conducting sheath helix winding on its core-cladding boundary. A simple analytical method using the vector boundary conditions has been utilized to get the modal eigen value equation. From this equation dispersion curves are obtained and plotted for some particular values of the pitch angles of the winding. Next, these predicted results are compared with those of a new optical fiber having a conducting sheath helix winding on its core-cladding boundary. It is seen that the cutoff values are somewhat lower for the Piet Hein lightguide than those for the circular guide. This is not unexpected since the Piet Hein curve approaches the shape of a square. The

introduction of a conducting helical winding leads to a modification of the modal characteristics of the lightguides and gives us an additional means to control them.

1. INTRODUCTION

The conventional optical fiber having a circular core cross-section which is widely used in optical communication systems [1–3]. But unconventional optical waveguides having non-circular core cross-sections like elliptical, rectangular, triangular, Piet Hein hypocycloidal, cardioidic cross-sections etc. [4–12] have also been studied with a view to their possible use in integrated optical devices such as wavelength filtering, coupling, semiconductor laser technology and optical sensors.

Recently metal-clad optical waveguides [13–18] have been studied theoretically, experimentally and technically because these provide potential applications, such as connecting the optical components to other circuits, protecting the optical devices against stray light and heat sinking. Metallic -cladding structure on an optical waveguide is known as a TE-mode pass polarizer and is commercially applied to various optical devices [16, 17].

More recently the authors [19] investigated the modal behaviour of an unconventional optical waveguide having a core cross-section with a new type of asymmetric loop boundary. This waveguide sustains only a few modes, which is interesting and new in view of the generally known result that distortion usually leads to an increase in the number of sustained modes. The selection of such new types of unconventional cross-sections [10–12] is not random and arbitrary but systematic. Many of the geometries are the modifications or distortions of the circular and rectangular cross-sections. The Piet Hein geometry stands midway between the two. Also, the structures are chosen when a mathematical analysis becomes feasible. The basic idea is to see how a distortion of the cross-section or the introduction of a new material may change the modal characteristics, such as the number of guided modes sustained by the waveguide.

The relevance of this kind of analytical work is two-fold. It provides us with the technique of treating very difficult problems in an introductory way as a first step to obtain a basic insight so that it may lead to more precise and elaborate analysis as a second step. Also it is expected that theoretical work of this kind will provide the modal characteristics of a variety of lightguides having a rich fund of results from which technologists and researchers working in practical fields can choose the required characteristics and structures in future when the

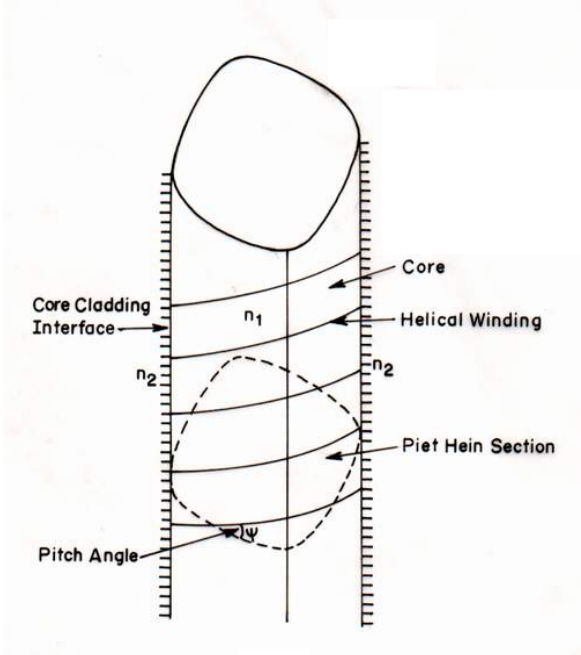

Figure 1. The Piet Hein lightguide with a conducting helical winding having the core refractive index n_1, the cladding of refractive index n_2 and the helical pitch angle ψ.

necessary fabrication technology becomes available. The possibility of fabrication, if not already there, is not remote in view of current advances in nanotechnology, if only the experimentalists are sufficiently interested or encouraged to take up this sort of work.

In this paper we consider a lightguide with new geometrical and structural features. The cross-section of the core-cladding interface is a Piet Hein curve which in shape stands midway between a circle and a square. On this core-cladding interface we introduce a conducting sheath helical winding Fig. 1. The modal characteristics of such a waveguide are next analytically obtained. For the sake of comparison, we also obtain the modal characteristics of the conventional circular fiber; on the core cladding interface of this fiber also we introduce a conducting helical winding Fig. 2.

The winding is right-handed and the direction of propagation is positive z direction. The winding angle of the helix ψ can take any arbitrary value between 0 to $\pi/2$. But for left-handed winding, ψ can be replaced by $(\pi - \psi)$.

The idea of a helical optical waveguide [20, 21] in the field of optical fiber technology stems from the travelling wave tube technology

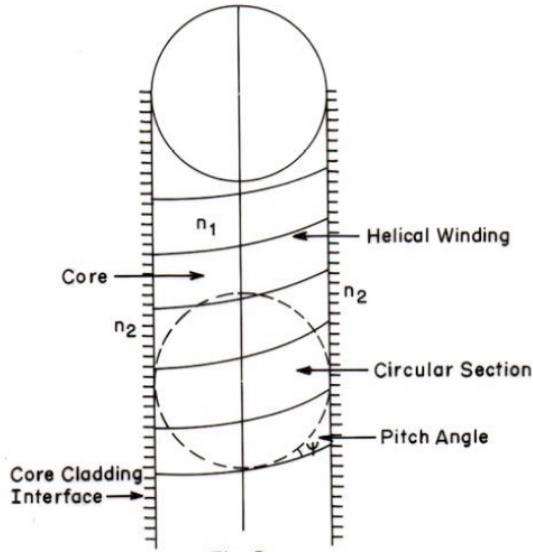

Figure 2. The standard circular optical fiber with a conducting helical winding having core refractive index n_1, the cladding of refractive index n_2 and the helical pitch angle ψ.

(TWT) in the microwave region [22, 23]. In that field, however, slow wave structures are used. We consider fast wave structures. The sheath helix can be obtained when many similar insulated and tight conducting windings are made side by side. This will be possible in an integrated way by using nanotechnology. In this case the property of conduction is only in the helical direction but not in the perpendicular direction. The periodicity of the structure will, as we shall see later, introduce band gaps and thus this waveguide may be placed in the category of photonic band gap structures which are currently receiving much attention.

2. THEORETICAL CONSIDERATIONS

2.1. The Piet Hein Lightguide with the Conducting Winding

The Cross sectional view of the Piet Hein waveguide is shown in Fig. 1. This shape in the general case represented by the equation

$$\left(\frac{x}{a}\right)^N + \left(\frac{y}{b}\right)^N = 1 \tag{1}$$

where N can take any integral values exceeding 2 and a and b are the semidiameters of the curve. For $N = 2$ the Piet Hein curve degenerates into an ellipse. For this reason the curve is some times called a super ellipse. For our modal analysis, to be specific, we have chosen $N = 4$. To simplify the algebra, we choose the special case $a = b = \rho$.

In this case we have

$$x^4 + y^4 = \rho^4 \tag{2}$$

where ρ is a parameter related to the size of the Piet Hein core cross-section. If we treat ρ as a variable, equation (1) represents a set of Piet Hein curves with $0 < \rho < \infty$. We next introduce a new coordinate system in which the coordinates of a point are determined by the intersection of two sets of curves; one set given by equation (1) and the other set being the set of curves normal to the first set. The set of normal curves is given by

$$\frac{1}{x^2} - \frac{1}{y^2} = \frac{1}{\xi^2} \tag{3}$$

where ξ is to be treated as a new coordinate variable. If we fix the value of ρ, we have a fixed curve. Using the new coordinates and Maxwell equations we can obtain the expressions for the field E and H in terms of the new coordinates. The details of this procedure are given in a previous paper by the authors [24]. The longitudinal components of the fields for the even modes, as a first approximation, can be written as

$$\left.\begin{aligned} E_{z1} &= AJ_1(Ud\rho)F(\xi)e^{j(\omega t-\beta z)} \quad (4)\\ H_{z1} &= BJ_1(Ud\rho)F(\xi)e^{j(\omega t-\beta z)} \quad (5)\end{aligned}\right\} \text{core region}$$

$$\left.\begin{aligned} E_{z2} &= CK_1(Wd\rho)F(\xi)e^{j(\omega t-\beta z)} \quad (6)\\ H_{z2} &= DK_1(Wd\rho)F(\xi)e^{j(\omega t-\beta z)} \quad (7)\end{aligned}\right\} \text{cladding region}$$

where $U^2 = \omega^2\mu\varepsilon_1 - \beta^2$ and $W^2 = \beta^2 - \omega^2\mu\varepsilon_2$. Here β is the axial component of propagation vector, ω is the wave frequency, μ is the permeability of non-magnetic medium, ε_1 and ε_2 are the permittivity of the core and the cladding region respectively. Also d is a number $(\sqrt{2})^{\frac{1}{2}}$ which emerges in the analysis because of the peculiarity of the geometrical shape and A, B, C and D are unknown constant to be determinant. We also write the expressions for the tangential electrical field components $E_{\xi 1}$, $H_{\xi 1}$, $E_{\xi 2}$, $H_{\xi 2}$ and also those for the radial field components $E_{\rho 1}$, $H_{\rho 1}$, $E_{\rho 2}$, $H_{\rho 2}$.

$$E_{\xi 1} = \frac{-j}{\omega^2\mu\varepsilon_1 - \beta^2}\left[j\frac{\beta\nu}{\rho}AJ_1(Ud\rho) - \mu_1\omega UdBJ_1'(Ud\rho)\right]F(\xi)e^{j(\omega t-\beta z)} \tag{8}$$

$$H_{\xi 1} = \frac{-j}{\omega^2\mu\varepsilon_1 - \beta^2}\left[j\frac{\beta\nu}{\rho}BJ_1(Ud\rho) + \omega\varepsilon_1 UdAJ_1'(Ud\rho)\right]F(\xi)e^{j(\omega t-\beta z)} \quad (9)$$

$$E_{\xi 2} = \frac{-j}{\beta^2 - \omega^2\mu\varepsilon_2}\left[j\frac{\beta\nu}{\rho}CK_1(Wd\rho) - \mu_2\omega WdDK_1'(Wd\rho)\right]F(\xi)e^{j(\omega t-\beta z)} \quad (10)$$

$$H_{\xi 2} = \frac{-j}{\beta^2 - \omega^2\mu\varepsilon_2}\left[j\frac{\beta\nu}{\rho}DK_1(Wd\rho) + \omega\varepsilon_2 WdCK_1'(Wd\rho)\right]F(\xi)e^{j(\omega t-\beta z)} \quad (11)$$

Here $F(\xi)$ is a function of the coordinate ξ satisfying the symmetries of the shape. Obviously ρ and ξ are analogous to the polar circular coordinates r and φ respectively.

As stated in our earlier paper [24] these equation are more reliable near the corner region, than in region far from corners. In order to have a guided field the following condition must be satisfied $n_1k_0 > \beta > n_2k_0$, where n_1 and n_2 are the refractive indices of the core region and cladding regions respectively and k_0 is the free space propagation constant. The boundary conditions demand that the tangential components of the electric field $\vec{E}$ and the magnetic field $\vec{H}$ at the interface should be continuous. In this structure, we use the sheath helix cladding region.

The electric field along the direction of winding determined by the pitch angle ψ should be zero. Thus we must have

$$E_{z1}\sin\psi + E_{\xi 1}\cos\psi = 0 \quad (12)$$

$$E_{z2}\sin\psi + E_{\xi 2}\cos\psi = 0 \quad (13)$$

The electric field components normal to the direction of winding are assumed to be continuous. Thus

$$E_{z1}\cos\psi - E_{\xi 1}\sin\psi = E_{z2}\cos\psi - E_{\xi 2}\sin\psi \quad (14)$$

$$H_{z1}\sin\psi + H_{\xi 1}\cos\psi = H_{z2}\sin\psi + H_{\xi 2}\cos\psi \quad (15)$$

Using the above expressions for the field components and the boundary conditions, four equation are obtained involving four unknown constants, which will yield a non-trivial solution if the determinant whose elements are the coefficients of these unknown constants is set equal to zero. Thus we have

$$\begin{vmatrix} A_{11} & A_{12} & A_{13} & A_{14} \\ A_{21} & A_{22} & A_{23} & A_{24} \\ A_{31} & A_{32} & A_{33} & A_{34} \\ A_{41} & A_{42} & A_{43} & A_{44} \end{vmatrix} = 0 \quad (16)$$

where

$$
\begin{aligned}
A_{11} &= J_1(Ud\rho)\left[\sin\psi + \frac{\beta}{\rho U^2}\cos\psi\right] \\
A_{12} &= \frac{j\omega\mu_1 d J_1'(Ud\rho)\cos\psi}{U} \\
A_{13} &= 0 \\
A_{14} &= 0 \\
A_{21} &= 0 \\
A_{22} &= 0 \\
A_{23} &= K_1(Wd\rho)\left[\sin\psi + \frac{\beta\nu}{\rho W^2}\cos\psi\right] \\
A_{24} &= \frac{j\omega\mu_2 d K_1'(Wd\rho)\cos\psi}{W} \\
A_{31} &= J_1(Ud\rho)\left[\cos\psi - \frac{\beta\nu}{\rho U^2}\sin\psi\right] \\
A_{32} &= -\frac{j\omega\mu_1 d J_1'(Ud\rho)\sin\psi}{U} \\
A_{33} &= -K_1(Wd\rho)\left[\cos\psi - \frac{\beta\nu}{\rho W^2}\sin\psi\right] \\
A_{34} &= \frac{j\omega\mu_2 d K_1'(Wd\rho)\sin\psi}{W} \\
A_{41} &= -\frac{jd\omega\varepsilon_1 J_1'(Ud\rho)\cos\psi}{U} \\
A_{42} &= J_1(Ud\rho)\left[\sin\psi + \frac{\beta\nu}{\rho U^2}\cos\psi\right] \\
A_{43} &= \frac{jd\omega\varepsilon_2 K_1'(Wd\rho)\cos\psi}{W} \\
A_{44} &= -K_1(Wd\rho)\left[\sin\psi + \frac{\beta\nu}{\rho W^2}\cos\psi\right]
\end{aligned}
$$

Expanding the determinant and after some simplification, one can have finally the following characteristic eigen value equation for the lowest order guided modes.

$$
\begin{aligned}
&U\frac{J_1(Ud\rho)}{J_1'(Ud\rho)}\left(\sin\psi + \frac{\nu\beta}{U^2\rho}\cos\psi\right)^2 - W\frac{K_1(Wd\rho)}{K_1'(Wd\rho)}\left(\sin\psi + \frac{\nu\beta}{W^2\rho}\cos\psi\right)^2 \\
&\quad -k_0^2 n_1^2 \frac{d^2}{U}\frac{J_1'(Ud\rho)}{J_1(Ud\rho)}\cos^2\psi + k_0^2 n_2^2 \frac{d^2}{W}\frac{K_1'(Ud\rho)}{K_1(Ud\rho)}\cos^2\psi = 0 \qquad (17)
\end{aligned}
$$

2.2. The Circular Fiber with Conducting Windings

The guided modes along this type of fiber can be analysed in a standard way, with a cylindrical system of co-ordinates (r, φ, z) assuming a harmonic time and z-dependence $e^{j(\omega t-\beta z)}$ of the fields. In order to have a guided field the following condition must be satisfied $n_1 k_0 > \beta > n_2 k_0$, where n_1 and n_2 are the refractive indices of the core region and the cladding regions respectively. The solution of the axial field components can now be written as

$$\left.\begin{aligned} E_{z1} &= AJ_\nu(Ua)F(\xi)e^{j(\omega t-\beta z)} \quad (18)\\ H_{z1} &= BJ_\nu(Ua)F(\xi)e^{j(\omega t-\beta z)} \quad (19)\end{aligned}\right\}\text{core region}$$

$$\left.\begin{aligned} E_{z2} &= CK_\nu(Wa)F(\xi)e^{j(\omega t-\beta z)} \quad (20)\\ H_{z2} &= DK_\nu(Wa)F(\xi)e^{j(\omega t-\beta z)} \quad (21)\end{aligned}\right\}\text{cladding region}$$

The transverse components can be obtained by using Maxwell's standard relations. The electric and magnetic field components E_ϕ and H_ϕ for each region can be written as

$$E_{\phi 1} = \frac{-j}{\omega^2\mu\varepsilon_1-\beta^2}\left[j\frac{\beta\nu}{a}AJ_1(Ua)-\mu_1\omega UBJ_1'(Ua)\right]F(\xi)e^{j(\omega t-\beta z)} \quad (22)$$

$$H_{\phi 1} = \frac{-j}{\omega^2\mu\varepsilon_1-\beta^2}\left[j\frac{\beta\nu}{a}BJ_1(Ua)+\omega\varepsilon_1 UAJ_1'(Ua)\right]F(\xi)e^{j(\omega t-\beta z)} \quad (23)$$

$$E_{\phi 2} = \frac{-j}{\beta^2-\omega^2\mu\varepsilon_2}\left[j\frac{\beta\nu}{a}CK_1(Wa)-\mu_2\omega WDK_1'(Wa)\right]F(\xi)e^{j(\omega t-\beta z)} \quad (24)$$

$$H_{\phi 2} = \frac{-j}{\beta^2-\omega^2\mu\varepsilon_2}\left[j\frac{\beta\nu}{a}DK_1(Wa)+\omega\varepsilon_2 WCK_1'(Wa)\right]F(\xi)e^{j(\omega t-\beta z)} \quad (25)$$

By using the above boundary conditions for conducting sheath helix equations (12) to equation (15) and by using equations (18) to equations (25), we can get the following characteristic equation for the lowest order guided modes.

$$U\frac{J_1(Ua)}{J_1'(Ua)}\left(\sin\psi+\frac{\nu\beta}{U^2a}\cos\psi\right)^2 - W\frac{K_1(Wa)}{K_1'(Wa)}\left(\sin\psi+\frac{\nu\beta}{W^2a}\cos\psi\right)^2 - \frac{k_0^2n_1^2}{U}\frac{J_1'(Ua)}{J_1(Ua)}\cos^2\psi+\frac{k_0^2n_2^2}{W}\frac{K_1'(Ua)}{K_1(Ua)}\cos^2\psi = 0 \quad (26)$$

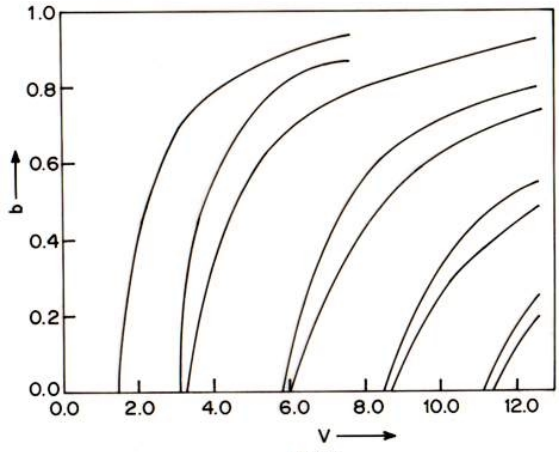

Figure 3. Dispersion curves of normalized propagation constant (b) versus normalized frequency parameter V for pitch angle $\psi = 0^\circ$ (Piet Hein lightguide).

3. NUMERICAL RESULTS AND DISCUSSIONS

We now make some sample computations based on equation (17) and equation (26). We choose $n_1 = 1.50,\ n_2 = 1.46,\ \lambda_0 = 1.55 \times 10^{-6}\,\mathrm{m}$ and plot some dispersion curves which are shown in Fig. 3 to Fig. 12. Here we have introduced two dimensionless parameters b and V, as is usually done. We have $b = \frac{\frac{\beta^2}{k_0^2} - n_2^2}{n_1^2 - n_2^2}$ =normalized propagation constant and $V = \frac{2\pi a}{\lambda_0}(n_1^2 - n_2^2)^{\frac{1}{2}}$ = normalized frequency parameter. We also obtain the cutoff-values for the same modes which can be seen directly from the dispersion curves or obtained from the cutoff equations, easily derivable from equation (17) and equation (26) by allowing W to tend to zero. These values and their dependence on the helical pitch angle ψ can be seen for the two lightguides in Table 1 and Table 2.

We want to draw the reader's attention to some interesting features of the dispersion curves shown in Fig. 3 to Fig. 12. They all have the standard expected shape, but except for the lowest order modes, they come in pairs, that is, the cutoff values for two adjacent modes converge. This means that one effect of the conducting winding is to split the modes and remove a degeneracy which is hidden in conventional lightguides without these windings. Although we have not studied polarization in this paper, this implies that the helical winding

Table 1. Cutoff V_c-values for some low order modes ($\nu = 1$) for different values of the pitch angle ψ. (Piet Hein waveguide with helical winding).

S.No.	ψ =0	ψ =30°	ψ =45°	ψ =60°	ψ =90°
1.	1.489	0.042	0.069	0.167	1.562
2.	3.111	1.534	1.394	1.255	3.208
3.	3.236	1.553	3.099	1.563	4.603
4.	5.858	3.110	3.099	3.096	5.900
5.	5.928	3.264	5.858	3.097	7.253
6.	8.523	5.858	5.998	5.845	8.648
7.	8.648	5.928	8.648	5.928	9.904
8.	11.381	8.643	8.649	8.632	11.299
9.	11.382	8.648	11.428	8.634	12.554
10.	-	11.142	11.438	11.381	-
11.	-	11.143	-	11.382	-

Table 2. Cutoff V_c-values for some low order modes ($\nu = 1$) for different values of the pitch angle ψ. (circular fiber with helical winding).

S.No.	ψ =0	ψ =30°	ψ =45°	ψ =60°	ψ =90°
1.	1.771	0.065	0.394	0.278	1.855
2.	3.702	1.673	1.673	1.534	3.808
3.	3.905	1.855	1.855	1.869	5.440
4.	6.974	3.693	3.688	3.682	7.016
5.	7.114	3.905	3.696	3.905	8.648
6.	10.183	6.974	6.974	6.974	10.183
7.	10.322	7.164	7.250	7.142	11.857
8.	-	10.183	10.183	10.183	-
9.	-	10.322	10.280	10.322	-

possibly introduces important changes in polarization properties. This we except to consider in a future study.

We also observe that another effect of the conducting helical winding is to reduce the cutoff values for the circular fiber, thus in increasing the number of modes. This effect is undesirable for the possible use of these lightguides for long distance communication, but may be usefully exploited if one is interested in devices with

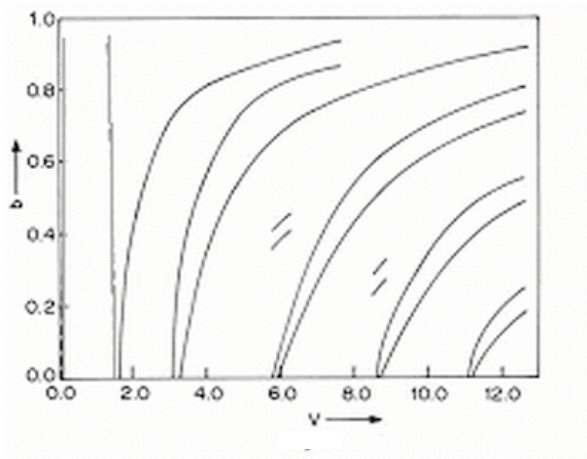

Figure 4. Dispersion curves of normalized propagation constant (b) versus normalized frequency parameter V for pitch angle $\psi = 30°$ (Piet Hein lightguide).

particular properties. Also the cutoff values are somewhat smaller for the Piet Hein shape than for the circular shape. This feature is also expected since the Piet Hein shape approaches the square and it is well known that rectangular waveguides have lower modal cutoff values than circular waveguides. The Piet Hein shape therefore will be suitable for application in integrated optical devices and will have the advantage that since they have no corner discontinuities will have lesser scattering problems.

An anomalous feature in the dispersion curves is observable for $\psi = 30°$, $45°$ and $60°$ for both types of lightguide [Fig. 4, Fig. 5, Fig. 6, Fig. 9, Fig. 10, Fig. 11] near the lowest order mode. It is found that on the left of the lowest cutoff values, portions of curves appear which have no resemblance with standard dispersion curves, and have no cutoff values. This means that for very small value of V (in particular small sizes) anomalous dispersion properties may occur in helically wound lightguides. In view of the complication of the structure, a simple physical explanation of this feature is not available. We are, however, more fortunate in the case of another apparent anomalous feature in some of the curves. We find that some curves have gaps of discontinuities between some values of V. These represent the band gaps or the forbidden bands of the structure. These are induced by the periodicity of the helical windings and are also found in slow wave structures [22]. As a matter of fact, these are expected and entitle our waveguide to be put into the category of the photonic band gap

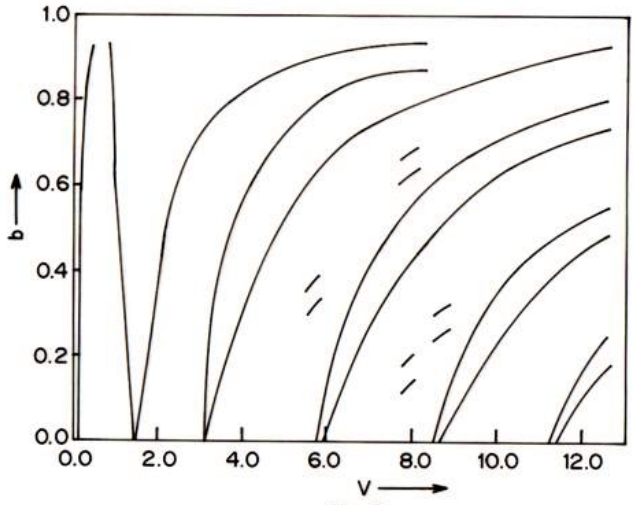

Figure 5. Dispersion curves of normalized propagation constant (b) versus normalized frequency parameter V for pitch angle $\psi = 45°$ (Piet Hein lightguide).

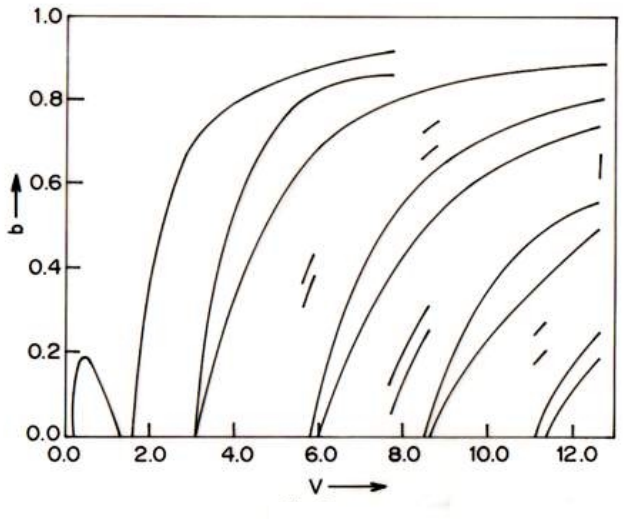

Figure 6. Dispersion curves of normalized propagation constant (b) versus normalized frequency parameter V for pitch angle $\psi = 60°$ (Piet Hein lightguide).

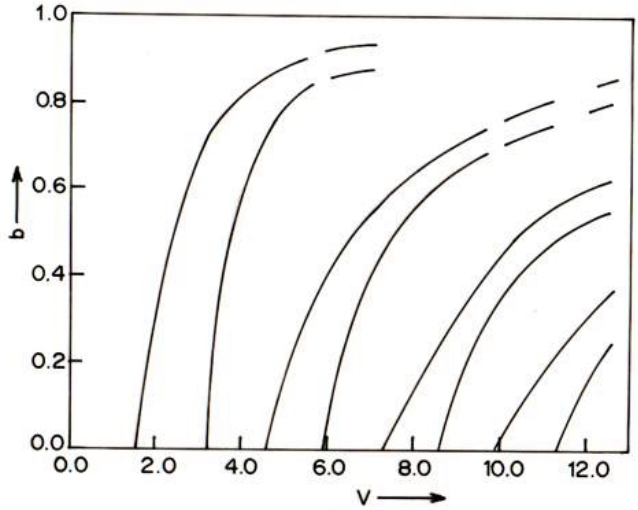

Figure 7. Dispersion curves of normalized propagation constant (b) versus normalized frequency parameter V for pitch angle $\psi = 90^\circ$ (Piet Hein lightguide).

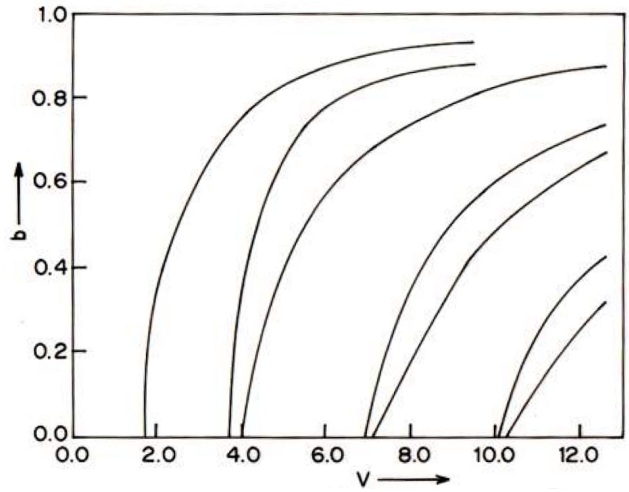

Figure 8. Dispersion curves of normalized propagation constant (b) versus normalized frequency parameter V for pitch angle $\psi = 0^\circ$ (Circular fiber).

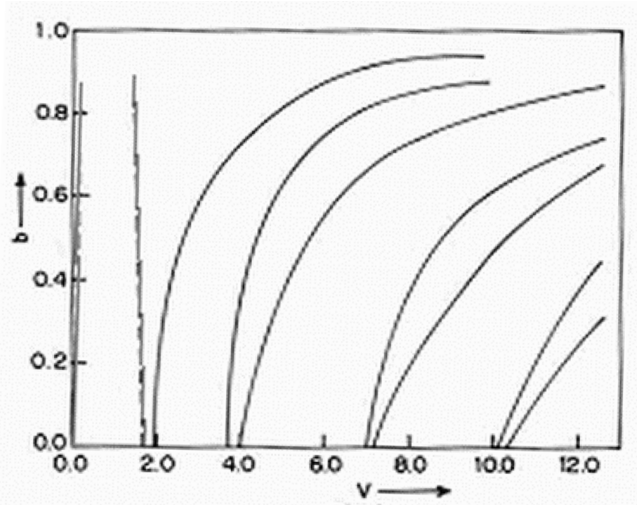

Figure 9. Dispersion curves of normalized propagation constant (b) versus normalized frequency parameter V for pitch angle $\psi = 30^\circ$ (Circular fiber).

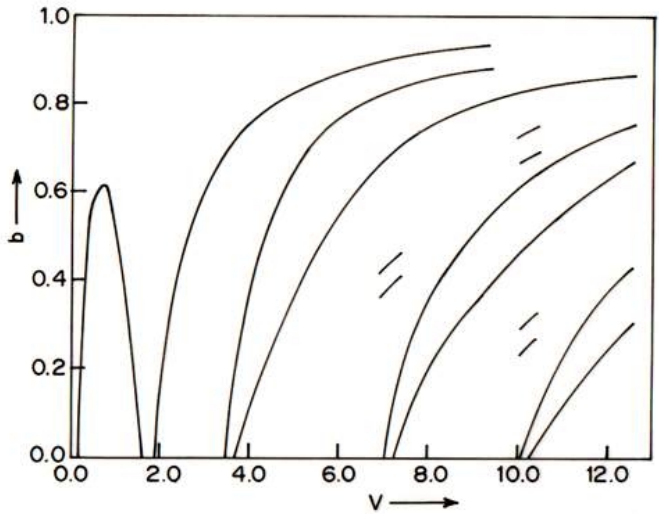

Figure 10. Dispersion curves of normalized propagation constant (b) versus normalized frequency parameter V for pitch angle $\psi = 45^\circ$ (Circular fiber).

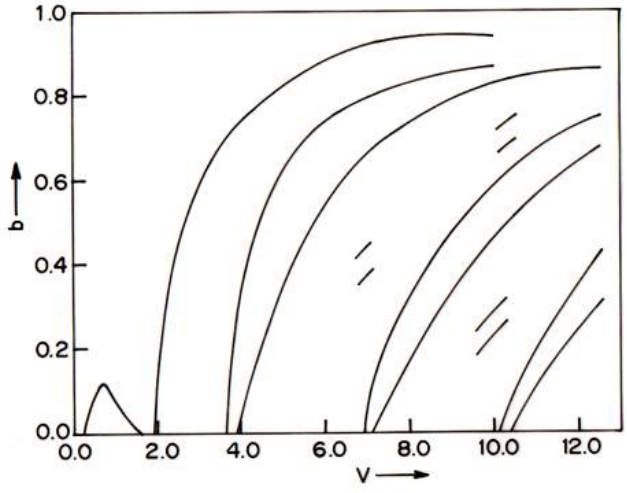

Figure 11. Dispersion curves of normalized propagation constant (b) versus normalized frequency parameter V for pitch angle $\psi = 60^\circ$ (Circular fiber).

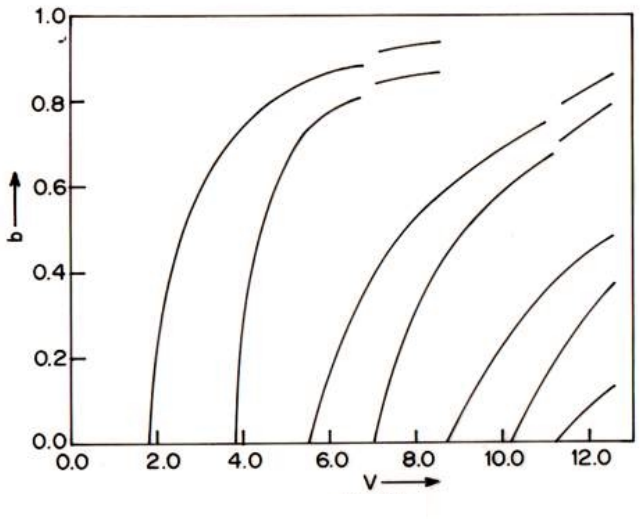

Figure 12. Dispersion curves of normalized propagation constant (b) versus normalized frequency parameter V for pitch angle $\psi = 90^\circ$ (Circular fiber).

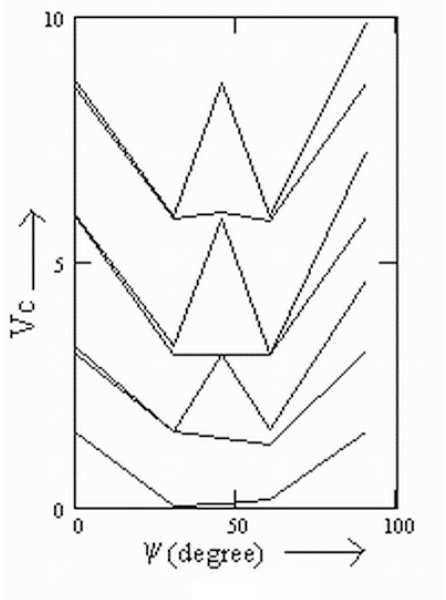

Figure 13. The dependence of the cutoff values V_c on the pitch angle ψ, for Piet-Hein optical waveguide.

structures [26, 27].

We now come to Table 1 and Table 2. We note particularly that the dependence of the cutoff V-value (V_c) on ψ is such that as ψ is increased, there is a drastic fall in V_c at $\psi = 30^\circ$ and then a small increase as ψ goes from 30° to 60° ; then there is a quick rise as ψ changes from 60° to 90°. Thus the two most sensitive regions in respect of the influence of the helical pitch angle ψ on the cutoff values and the modal properties of lightguides are the ranges $\psi = 0^\circ$ to $\psi = 30^\circ$ and $\psi = 60^\circ$ to $\psi = 90^\circ$ and it is in these ranges the new lightguides are expected to have potential applications with ψ as a means for controlling the modal properties. Incidentally, the anomalous dispersion curves do not appear in these ranges of ψ values. For a clearer understanding of the dependence of the cutoff values V_c on the pitch angle ψ, we supplements Table 1 and Table 2 by the corresponding graphical representations Fig. 13 and Fig. 14. Table 1 and Table 2 are still important in view of the computational values they show.

In this paper our main interest has been on the modal behaviour. We are aware that the field distribution of the modal field is of considerable importance and we hope to present this aspect in a future communication.

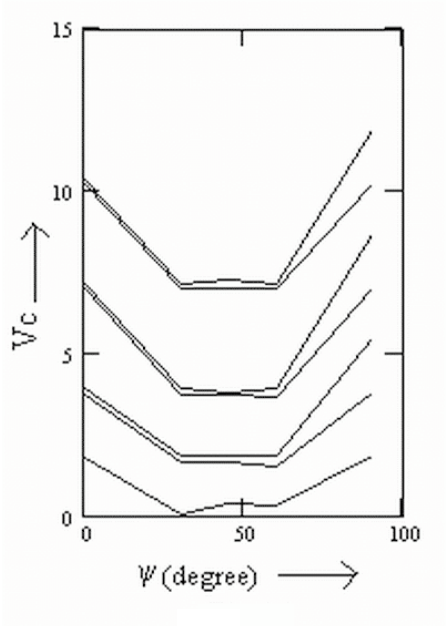

Figure 14. The dependence of the cutoff values V_c on the pitch angle ψ, for circular fiber.

ACKNOWLEDGMENT

We are grateful to Prof. P. Khastgir for his kind help and encouragement through out the work.

REFERENCES

1. Clarricoats, P. J. B., "Propagation along bounded and unbounded dielectric rods," *IEEE Monograph 409E*, 1960.
2. Snitzer, E., "Cylindrical dielectric waveguide modes," *J. Opt. Soc. Am.*, Vol. 51, 491–498, 1961.
3. Miller, S. E., E. A. J. Marcatili, and T. Li, "Research towards optical fiber transmission systems, Part I: The transmission medium," *Proc. IEEE*, Vol. 61, 1703–1751, 1973.
4. Kumar, A., V. Thyagaranjan, and A. K. Ghatak, "Analysis of rectangular core dielectric waveguides: An accurate perturbation approach," *Opt. Lett.*, Vol. 8, 63–65, 1983.
5. Yeh, C., "Elliptical dielectric waveguide," *J. Appl. Phys.*, Vol. 33, 3235–3242, 1962.

6. Yeh, C., "Modes in weakly guiding elliptical optical fibers," *Opt. Quantum Electron*, Vol. 8, 43–47, 1976.
7. Dyott, R. B., "Cutoff of the first order modes in elliptical dielectric waveguide: An experimental approach," *Electron Lett.*, Vol. 26, 1721–1723, 1990.
8. Dyott, R. B., "Glass-fiber waveguide with triangular core," *Electron Lett.*, Vol. 9, 288–290, 1973.
9. James, J. R. and I. N. L. Gallett, "Modal analysis of triangular cored fiber waveguide," *Proc. IEEE*, Vol. 120, 1362–1370, 1973.
10. Mishra, V., "A study on Peit Hein and other unconventional geometry in optical waveguides," Ph.D. Thesis, Applied. Phys. I.T. B.H.U., India, 1997.
11. Rao, M. P. S., B. Prasad, P. Khastgir, and S. P. Ojha, "Modal cutoff conditions for an optical waveguide with a hypocycloidal cross section," *Microwave Opt. Technol. Lett.*, Vol. 14, 177–180, 1997.
12. Rao, M. P. S., V. Singh, B. Prasad, P. Khastgir, and S. P. Ojha, "An analytical study of the dispersion curves of an annular waveguide made of liquid crystal," *Photonics and Optoelectronics*, Vol. 5, 73–78, 1998.
13. Kaminow, I. P., W. L. Mammel, and H. P. Weber, "Metal clad optical waveguides: analytical and experimental study," *Appl. Optics*, 396–405, 1974.
14. Polky, J. N. and G. L. Mitchell, "Metal clad planar dielectric waveguide for integrated optics," *J. Opt. Soc. Am.*, Vol. 64, 274–279, 1974.
15. Rollke, K. H. and W. Sohler, "Metal clad waveguides as cutoff polarizer for integrated optics," *IEEE J. Quantum Electron*, Vol. QE-13, 141–145, 1972.
16. Sletten, M. and S. Seshadri, "Thick metal surface-polariton polarizor for a planar optical waveguide," *J. Opt. Soc. Am.*, Vol. 7, 1174–1184, 1990.
17. Sletten, M. and S. Seshadri, "Experimental investigation of a thin film surface polariton polarizor," *J. Appl. Phys.*, Vol. 70, 574–579, 1991.
18. Rao, M. P. S., B. Prasad, and S. P. Ojha, "Theoretical study of thin circular infrared filter with alternate concentric regions of dielectric and partially conducting materials," *Photonis and Optoelectronics*, Vol. 2, 157–167, 1994.
19. Singh, V., B. Prasad, and S. P. Ojha, "Weak guidance analysis and dispersion curves of an infrared lightguide having a core cross-

section with a new types of asymmetric loop boundary," *Optical Fiber Technology*, Vol. 6, 290–298, 2000.

20. Bunch, K. J. and R. W. Grow, "The helically wrapped circular waveguide," *IEEE. Trans. Electron. Devices*, Vol. ED-34, 1873–1885, 1987.
21. Kumar, D., "Propagation characteristics of helical cladding elliptical step index fiber," Ph.D. Thesis, Applied. Phys. I.T. B.H.U., India, 1999.
22. Watkins, D. A., *Topics in Electromagnetic Theory*, 39–62, Wiley, New York, 1958.
23. Pierce, J. R., *Travelling Wave Tubes*, 229–230, Van Nostrand, New York, 1950.
24. Singh, V., B. Prasad, and S. P. Ojha, "Theoretical analysis and dispersion curves of an annular lightguide with a cross section bounded by two Piet Hein curves," *J. of Electromagn. Waves and Appl.*, Vol. 17, 1025–1036, 2003.
25. Singh, V., B. Prasad, and S. P. Ojha, "A comparative study of modal characteristic and waveguide dispersion of optical waveguide with three different closed loop cross sectional boundaries," *Optik*, Vol. 115, 281–288, 2004.
26. Yablonovitch, E., "Inhibited spontaneous emission in solid state and electronics," *Phys. Rev. Lett.*, Vol. 58, 2059–2062, 1987.
27. Joannoupoulos, J. D., R. D. Meade, and J. N. Winn, *Photonic Crystals: Molding the Flow of Light*, Princeton University Press, Princeton, NJ, 1995.